Reactive Uptake of N_2O_5 by Aerosols Containing Dicarboxylic Acids. Effect of Particle Phase, Composition, and Nitrate Content

Paul T. Griffiths,*,† Claire L. Badger,† R. Anthony Cox,† Mareike Folkers,‡ Hartmut H. Henk,‡ and Thomas F. Mentel‡

Centre for Atmospheric Science, Department of Chemistry, Lensfield Road, University of Cambridge, Cambridge, CB2 1EW, United Kingdom, and ICG-II, Forschungszentrum Jülich, D-52425 Jülich, Germany

Received: November 2, 2008; Revised Manuscript Received: February 4, 2009

Reactive uptake coefficients for loss of N_2O_5 to micron-size aerosols containing oxalic malonic, succinic, and glutaric acids, and mixtures with ammonium hydrogen sulfate and ammonium sulfate, are presented. The uptake measurements were made using two different systems: atmospheric pressure laminar flow tube reactor (Cambridge) and the Large Indoor Aerosol Chamber at Forschungszentrum Juelich. Generally good agreement is observed for the data recorded using the two techniques. Measured uptake coefficients lie in the range $5 \times 10^{-4}-3 \times 10^{-2}$, dependent on relative humidity, on particle phase, and on particle composition. Uptake to solid particles is generally slow, with observed uptake coefficients less than 1×10^{-3}, while uptake to liquid particles is around an order of magnitude more efficient. These results are rationalized using a numerical model employing explicit treatment of both transport and chemistry. Our results indicate a modest effect of the dicarboxylic acids on uptake and confirm the strong effect of particle phase, liquid water content, and particulate nitrate concentrations.

1. Introduction

Nitrogen oxides play an important role in controlling the oxidizing capacity of the troposphere, as, together with CO, methane and other volatile organic compounds (VOCs), NO_2, and NO control the photochemical cycles which produce OH and O_3. In addition, under conditions of low solar flux, concentrations of NO_3 radicals formed from the reaction of NO_2 and O_3 can reach significant levels and contribute to the rate of oxidation of VOCs. This has implications for nighttime oxidation chemistry, where NO_3 is thought to play a controlling role. Heterogeneous removal of the NO*x* reservoir species, N_2O_5, via reaction R1 therefore has an important effect on the rate of oxidation of VOCs and on ozone levels in the troposphere.

$$N_2O_{5(g)} + H_2O_{(liq)} \xrightarrow{\text{aerosol}} 2HNO_{3(aq)} \qquad \text{(R1)}$$

A number of studies have been made of the kinetics of N_2O_5 uptake onto aerosol particles, and the importance of relative humidity, particle phase, and composition has been identified.[1−6] Despite this, a number of outstanding issues remain, in particular the effect of temperature and of the composition of the aerosol. This study focuses on the role of organic compounds and particulate nitrate on uptake.

Our picture of effect of organic compounds on the aqueous reactivity of N_2O_5 in particles is still emerging. Surface-active organics appear to have a significant effect. Folkers et al. observed that the oxidation products of the biogenic alkene alpha-pinene reduce the uptake rate onto inorganic aerosols.[7] O'Neill et al. observed that uptake coefficients decrease with increasing surface coverage of species such as oleate: about an order of magnitude decrease in the rate of uptake is observed at or around monolayer coverage, indicating that the organic coating impedes one or more steps of the reactive uptake process.[8] Similar results were observed by Badger et al.[9] Recently, Nathanson and co-workers have demonstrated that the hydrolysis of N_2O_5 on sulfuric films is inhibited by coatings of hexanol and butanol.[10] In their study of the effect of thick layers of secondary organic material on aerosol uptake, Anttila et al. ascribe the reduction in uptake coefficient to the reduced solubility, transport, and rate of reaction of the N_2O_5 in the organic layer.[11]

As far as we are aware, uptake onto aerosol-containing organic species that are miscible with water has so far only been studied by Thornton et al., who measured the uptake of N_2O_5 by malonic acid and azelaic, nonan-1,9-dioic acid, aerosol over the range 10−85%.[12] Uptake to malonic acid was found to proceed at a rate comparable to inorganic salts and sulfuric acid, with uptake coefficients increasing from 0.005 to 0.03 with increasing relative humidity (RH). On the other hand, reactive uptake by the solid azelaic acid particles could not be observed, consistent with an uptake coefficient with an upper limit of $(5 \pm 3) \times 10^{-4}$.

Here we address uptake by aqueous aerosols containing several different dicarboxylic acids and, for the first time, their mixtures with ammonium sulfates. We have measured uptake by C_2-C_5 dicarboxylic acids (oxalic, malonic, succinic, and glutaric) which have been observed in tropospheric aerosol at the level of 0.2−3% mass of total organic carbon.[13] In addition N_2O_5 uptake on ammonium oxalate aerosols was measured.

Uptake measurements were made using two experimental techniques: the Large Indoor Aerosol Chamber at Forschungszentrum Juelich was used for a number of the measurements, while parallel, complementary work was performed using an atmospheric pressure aerosol flow tube in Cambridge. This has allowed a wide range of experimental parameters to be investigated, including relative humidity, particle size, and N_2O_5

* Corresponding author. E-mail: ptg21@cam.ac.uk.
† University of Cambridge.
‡ Forschungszentrum Jülich.

10.1021/jp8096814 CCC: $40.75
Published on Web 04/01/2009

mixing ratio. The data provide new information toward quantifying uptake by multicomponent aerosols, with the goal of allowing a more accurate representation within global atmospheric chemistry models.

2. Experimental Methods

2.1. Chamber Measurements. Measurements of reactive uptake were made using the Large Indoor Aerosol Chamber at Forschungszentrum Juelich. The construction and the operational performance of the aerosol chamber was described previously.[6,14] The chamber has a volume of 260 m^3 and a wall surface of 250 m^2 and is built as a double-wall system. A welded aluminum box serves as a gas-tight outside wall. Inside this box, a fully heat-sealed Teflon-FEP bag hangs from the ceiling and is spread by springs at the edges of the floor. The space between the aluminum walls and the Teflon-FEP bag is flushed continuously with 1 m^3/h synthetic air (Linde LiPur quality 6.0). This air stream is humidified by Milli-Q water to the level of relative humidity inside the chamber. The mixing in the chamber is provided by a floor heater which periodically switches between 20 and 30 °C water temperature. The chamber is cleaned directly after an experiment by flushing outside air with particle filters in line for at least 24 h. Before the next experiment the chamber is flushed for 24 h with a stream of ca. 30 m^3/h of clean synthetic air (Linde Lipur quality 6.0). The chamber is humidified to the desired relative humidity, here usually around 60%, by evaporation of Milli-Q water directly into the chamber. Relative humidity and temperature are measured at two positions in the chamber. In all model calculations described below, the average relative humidity and temperature are used.

Aerosol is generated by spraying dilute solutions of the aerosol substrates (typically 0.0625−0.13 M) via 10 2-fluid nozzles into a small prechamber. The fine fraction of the aerosol is flushed into the Large Aerosol Chamber by the generation air stream (140 L/min.). The final state of the aerosol is controlled by the relative humidity in the large aerosol chamber: metastable aerosols which remain liquid below their deliquescence point are generated if the relative humidity in the aerosol chamber is adjusted in between deliquescence and recrystallization point of the respective compound, by making use of the hysteresis effect in the Köhler curve. The number distribution of aerosol particles with diameters smaller than 500 nm is measured by a TSI SMPS3071/CPC3022A system. Particles larger than 700 nm are measured by a TSI APS3321 aerodynamic particle sizer in combination with a dilution stage (TSI 3302A). The aerosol composition in terms of sulfate, nitrate, and dicarboxylates is determined online by steam jet aerosol collection/ion chromatography (SJAC/IC).[15]

The concentrations of NO_2, N_2O_5, and HNO_3 were measured by in-chamber FTIR absorption spectroscopy (Bruker IFS120HR). Spectra were taken in the MIR range (5000−500 cm^{-1}). A resolution of 0.1 cm^{-1} was chosen which roughly corresponds to the pressure broadening of single rotational lines of water vapor at 1 atm. This way the gas-phase species were detected in between water lines, even at high relative humidity. Typically 18 or 36 scans per spectrum were taken, which enables a best time resolution of 90 s at a detection limit of about 11−17 ppb for NO*y* species on a 69 m optical path length (in-chamber White system). In these experiments N_2O_5 was formed in situ in the aerosol chamber by oxidation of NO_2 with O_3. Ozone was measured by an UV absorption monitor (Ansyco O3 41M). Temperature, relative humidity (Vaisala), and the pressure in the chamber (MKS-Baratron) are routinely recorded by a data-processing system.

The reaction probability γ is derived from the measured gas-phase concentrations and the measured aerosol distributions by kinetic model calculations. The box model consists of an evaluated gas-phase mechanism for the NO*x*/O_3/NO*y* chemistry and experimentally determined chamber specific wall loss terms.[6] A linear source term is used to simulate the addition of the second reactant O_3 into the chamber. The heterogeneous loss of N_2O_5 on the aerosol surface is included via reaction R2 which is based on simple gas kinetics:

$$N_2O_{5(g)} \xrightarrow{k_{het}} 2HNO_{3(aq)} \quad \text{(R2)}$$

$$k_{het} = \gamma \frac{c}{4} S_{tot}(t) \quad (1)$$

Herein c is the mean speed of N_2O_5 in the gas phase and $S_{tot}(t)$ the total aerosol surface density as a function of time calculated from the measured aerosol distributions, as described below. The parameter f gives the fraction of heterogeneously formed HNO_3 which is observable in the gas phase. The Fuchs−Sutugin correction proved to be negligible for the magnitudes of γ and the aerosol size distribution observed in this study. The experimental boundary conditions (temperature, pressure, relative humidity) and $S_{tot}(t)$ are constrained to the experimental data in the model calculations.

The reaction probability is determined by least-squares fitting the model to the observed N_2O_5 (t), NO_2 (t), and O_3 (t) with γ as a free parameter [FACSIMILE for Windows, Version 2.0.98, AEA Technology, plc 1998]. γ is essentially determined by the height and the appearance time of the N_2O_5 maximum which are defined by the known production rate of N_2O_5 from NO_2 and O_3 and the destruction rate on the aerosol surface, that for a given S_{tot} (and T) depends on the magnitude of γ only. The error in γ is generally dominated by the error in S_{tot} that is about ±10% for the combination of SMPS/APS with the evaluation procedure as described below.

The number size distributions observed in the aerosol chamber cover diameter ranges from roughly 20 nm to 5 μm. They are monomodal, slightly distorted log-normal distributions with typical count median diameters of about 120−140 nm and geometric standard deviations of 2.0−2.2. With increasing duration of the experiment, the size distributions in the chamber approach log-normal distributions. To derive S_{tot} from the measured particle size distributions, first the APS data with a time resolution of 300 s is linearly interpolated channel by channel to the time axis of the SMPS (time resolution of 400 s). To match the data from the two instruments, the aerodynamic diameter d_{ae} measured by the APS is then converted into the volume equivalent diameter d_p by the following relationship

$$d_p = d_{ae}\sqrt{\frac{\chi \rho_p C_{c,ae}}{\rho_0 C_{c,p}}} \quad (2)$$

where χ is the dynamic shape factor of the particle, $C_{c,ae}$ and $C_{c,p}$ are the slip correction factors for the aerodynamic diameter and the volume equivalent diameter, respectively, ρ_p is the particle density, and ρ_0 is equal to 1 g cm^{-3}. Since we studied liquid, thus spherical, particles in all experiments, the dynamic shape factor χ is equal to 1. For the purely inorganic systems, the required densities ρ_p as a function of the relative humidity are taken from single-particle levitation trap measurements

which also cover metastable droplets.[16] For the dicarboxylic acids and their mixtures with sulfates, such data for ρ_p are not available. To estimate ρ_p, the combined number size distributions from the SMPS and APS were fitted by a modified log-normal function, eq 3,[15] to find the optimal match in the range 300 nm to 1 μm. Therein ρ_p was allowed as an additional free parameter. Varying ρ_p only shifts the APS size distribution relative to the SMPS size distribution. This typically yields densities ρ_p for the metastable solutions of 1.2−1.5 g cm^{-3}.

The combined size distributions from the SMPS and APS are then converted to surface distributions and again fitted by the modified log-normal function

$$\frac{dS}{d\ln d_p} = A \exp\left[\frac{-\ln 2 \times \ln^2\left(1 + \frac{(\ln d_p - B)(D^2 - 1)}{C \times D}\right)}{\ln^2 D}\right] \quad (3)$$

and integrated over the whole size range to yield $S_{tot}(t)$ as a function of time. The parameters C and D in eq 3 determine the width and the asymmetry of the distribution, respectively. The distribution is positively skewed for $D > 1$ and negatively skewed for $D < 1$, respectively. For a typical particle size distribution in our chamber and particle densities of 1.35 g cm^{-3}, an overestimation of 10% in the particle density and thus incorrectly converted APS data results in an underestimation of about 6% in S_{tot}.

2.2. Aerosol Flow Tube Measurements. Kinetic measurements were also made using an atmospheric pressure aerosol flow tube. Submicron aerosols were generated using a TSI 3076 atomizer from aqueous solutions in deionized water. The aerosol was passed through a diffusion dryer (optional), and RH was controlled by dilution with a N_2 gas stream of variable RH. Aerosols consisted of either solid crystalline particles or deliquesced/metastable liquid droplets, depending on the RH and the properties of the aerosol (see below).

After adjustment of RH, the aerosol passed to a conditioner consisting of a temperature-controlled cylindrical tube after which point the aerosol flow was divided into two. A flow of 2800 cm^3 (STP) min^{-1} was used for aerosol characterization and the remainder (800 cm^3 (STP) min^{-1}) passed into the halocarbon wax-coated flow tube reactor (3.2 cm diameter × 65 cm length). Figure 1 shows a schematic of the experimental apparatus.

The aerosol was characterized using a differential mobility analyzer (DMA) (Hauke model EMS VIE-08) coupled to a Faraday cup electrometer (Hauke FCE-08A). The sheath airflow in the DMA was humidified to match the RH of the aerosol flow, thereby preventing any change in aerosol particle size during measurement. Figure 2 shows a typical size distribution obtained for malonic acid. Aerosol surface areas varied over the range 0.05−0.30 m^2 m^{-3}, with volumes of between 1 × 10^{-9} and 1 × 10^{-8} m^3 m^{-3} aerosol.

Kinetic measurements were made in the flow tube using a sliding injector to vary the contact time between N_2O_5 and the aerosol surface. For the flow conditions used, Reynolds numbers of between 20 and 40 are calculated and laminar flow is expected to develop after 5 s. The diffusion mixing time of N_2O_5 is also around 5 s. Accordingly, kinetics measurements were made over the range 5−40 s, the upper limit set by the length of our reactor of 70 cm.

First-order decays were observed under all conditions. Figure 3 shows the dependence of N_2O_5 concentration on residence

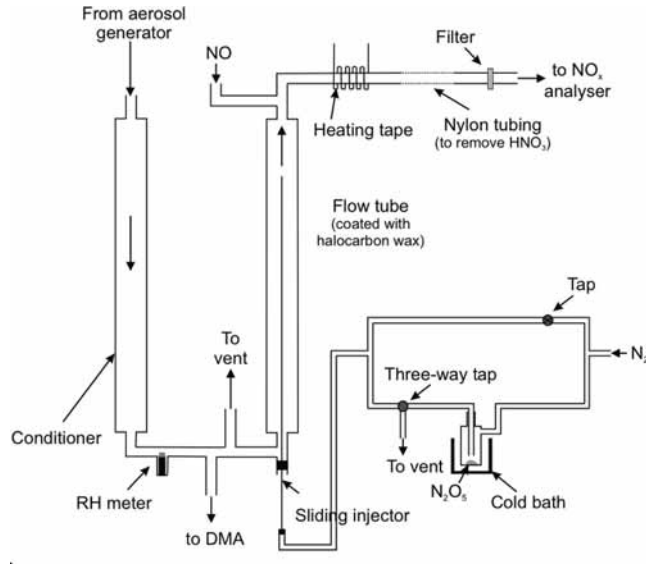

Figure 1. Aerosol flow tube system used to measure uptake coefficients for N_2O_5 hydrolysis on aerosol particles.

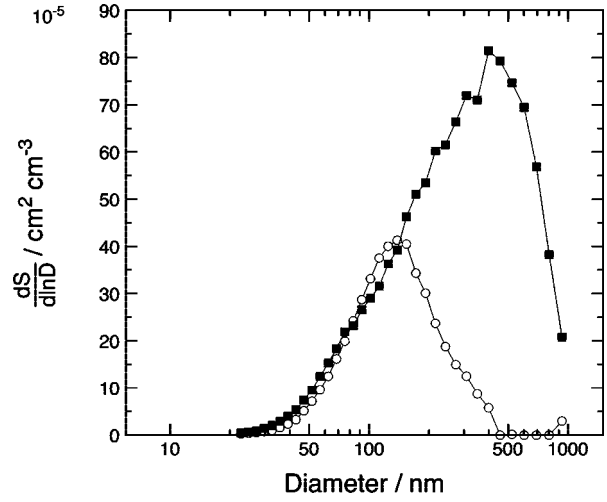

Figure 2. Surface area distributions as obtained using the DMA for malonic acid aerosol at two atomizer solution concentrations: ■, 0.01 M; ○, 0.1 M atomizer solution.

time in the flow tube. In general, significantly faster rates of decay are observed in the presence of aerosol. The rate of loss to the aerosol surface is derived from measurements of rates of decay in the presence and absence of aerosol using the procedures of Brown, as described elsewhere.[17] Mixing ratios of N_2O_5 in the flow tube were between 200 and 1000 ppbv.

Uptake coefficients, γ, were derived from the calculated rate of loss to the aerosol surface, k_{het}, using eq 1. Uptake coefficients were measured for aerosols comprising malonic, succinic, and glutaric acids, and for aerosols containing mixtures of these compounds with ammonium sulfate and ammonium hydrogen sulfate. Aerosols were generated from solutions of between 0.01 and 0.3 M concentration, the precise concentration used depending partly on the limited solubility of succinic acid in water of 86 g/L. Mixed aerosol was generated from solutions of 1:1 molar mixtures of varying concentration. Uptake coefficients were measured over a range of relative humidity from 30 to 75% RH.

3. Results

3.1. Uptake of N_2O_5 by Dicarboxylic Acid Aerosol. Table 1 lists the results of measurements of reactive uptake coefficients

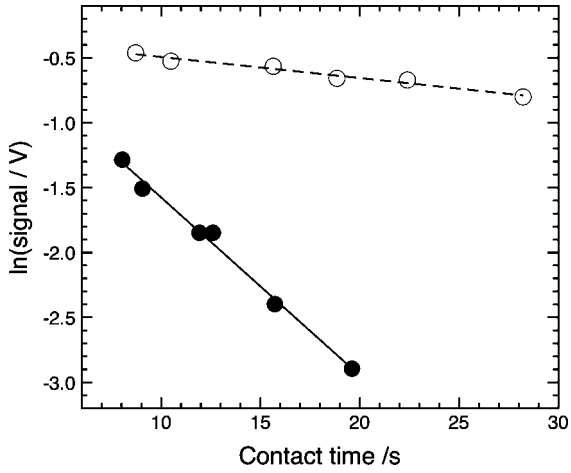

Figure 3. First-order plot for the loss of N_2O_5 to the flow tube walls in the absence of aerosol (open circles) and loss of N_2O_5 in the presence of aerosol. The lines show linear fits to the data from which the values for the first-order rate coefficients are calculated.

to dicarboxylic acid aerosols as a function of composition and RH. Figure 4 shows the uptake coefficients measured for the dicarboxylic acids over the range 30−75% RH. A general trend of increasing uptake with increasing RH is observed. Moderate uptake is observed under all conditions for malonic acid and glutaric acid, while for succinic acid a step change in reactivity is observed at 50% RH. At relative humidity below 50%, no measurable uptake was observed for this aerosol, and the uptake coefficients represent upper limits. Above 50% RH, the reactive uptake coefficients for glutaric and succinic acids are similar, being generally a factor of 2 lower than that to malonic acid aerosol.

The uncertainty in the γ arises from different sources in the two types of experiments. In the aerosol flow tube measurements, the uncertainty is derived from statistical errors in the fitting of the kinetic data. However, in the chamber measurements, the largest source of error arises from the assumptions regarding aerosol density used in the calculation of aerosol surface area from the measured SMPS and APS data. Accordingly, for the chamber measurements the lower bound was calculated assuming a density of 1.0 g cm^{-3}, and the upper by assuming a density of 1.6 g cm^{-3}.

Within the combined experimental uncertainty, good agreement is observed between the aerosol flow tube and chamber studies when similar experimental conditions are employed.

3.1.1. Uptake of N_2O_5 by Mixed Sulfate/Dicarboxylic Acid Aerosol. Uptake coefficients were measured at approximately 60% RH for mixed aerosol and are given in Table 2, with chamber measurements for comparison.

The agreement for the pure ammonium salts is excellent. Agreement between the two methods for the mixed systems is less satisfactory than in the other data set. In particular, uptake onto ammonium bisulfate/glutaric acids is somewhat lower as measured in the chamber, which may be explained partly by the lower relative humidity used. The uptake on the ammonium sulfate/glutaric aerosol is lower by about a factor of 2 in the AFT work, probably due to the larger particle size used in the chamber studies, as noted in the Discussion, and the slightly higher relative humidity. Uptake by ammonium sulfate/succinic acid is higher in the chamber measurements, but as discussed below, this may be due to the general inhibition of uptake by increasing experimental gas-phase N_2O_5 concentration.

4. Discussion

The findings presented in this study may be summarized quantitatively as follows: uptake by solid organic aerosol particles is very inefficient. For liquid aerosols, uptake coefficients increase with increasing RH and particle size (as measured using the ratio of aerosol volume to surface area). Uptake by the dicarboxylic acids is 30−90% of that by ammonium sulfate at similar RH. The effect of the organic acids on uptake by sulfate aerosols is small to moderate, being dependent on the organic acid, and uptake is roughly an order of magnitude faster than uptake to sulfate aerosols containing surface-active compounds.

While our understanding of the physical and chemical processes at work in the heterogeneous removal of N_2O_5 is still emerging, the current state of knowledge regarding uptake by inorganic aerosol particles is now quite robust: there is evidence that an ionic mechanism involving the nitronium ion, NO_2^+, or its hydrated form, and water is involved in the uptake process. The nitronium ion reacts further with water to make a protonated nitric acid, yielding an overall reaction of $N_2O_5 + H_2O \rightarrow 2HNO_3$, R1. Within the aerosol, the elementary steps involved are

$$N_2O_{5(g)} \rightarrow N_2O_{5(l)} \quad \text{(R3)}$$

$$N_2O_{5(l)} \rightarrow N_2O_{5(g)} \quad \text{(R4)}$$

$$N_2O_{5(aq)} \rightarrow NO^+_{2(aq)} + NO^-_{3(aq)} \quad \text{(R5)}$$

$$NO^+_{2(aq)} + NO^-_{3(aq)} \rightarrow N_2O_{5(l)} \quad \text{(R6)}$$

$$NO_2^+(aq) + H_2O_{(liq)} \rightarrow HNO_3 + H^+_{(aq)} \quad \text{(R7)}$$

$$HNO_3 \rightarrow NO_3^- + H^+_{(aq)} \quad \text{(R8)}$$

$$NO_3^- + H^+_{(aq)} \rightarrow HNO_3 \quad \text{(R9)}$$

There is considerable experimental evidence for this mechanism, including the measurements by Robinson et al. to aerosol comprising mixtures of sulfuric and nitric acid, as well as those of Wahner et al. to sodium nitrate aerosol and similar measurements by Hallquist et al.[4,6,18]

The mechanism proposes that the significant reduction in uptake coefficient with increasing nitrate activity in solution is the result of an increased rate of reaction R6. However, we demonstrate below that some quantitative information can be gleaned from a deeper analysis of our data in the context of other existing data sets.

The rate of reaction in solution affects the uptake coefficient. In general, for moderate rates of reactive uptake onto submicron aerosol, the reactive uptake coefficient is given by eq 4

$$\frac{1}{\gamma} = \frac{1}{\alpha} + \frac{c}{4K_H RT\sqrt{k_r D_l}} \frac{1}{[\coth q - 1/q]} \quad (4)$$

where α is the mass accommodation coefficient, c is the mean velocity of N_2O_5 molecules in the gas phase, K_H is the Henry's law constant for N_2O_5 in water, D_l is the liquid-phase diffusion

TABLE 1: Uptake Coefficients for N_2O_5 Hydrolysis, γ, Obtained for Aerosols Containing Dicarboxylic Acids[a]

aerosol	RH/%	$\gamma/10^{-3}$	V_a/S_a/nm	$[N_2O_5]$/ppbv	$[H_2O]$/M	comment
oxalic acid	**60**	<0.01	**180**	**830**	–	**efflorescent**
	74	$3.1^{+0.3}_{-1.2}$	**170**	**650**	–	**efflorescent**
malonic acid	30	8 ± 3	49	500	–	metastable
	50	12 ± 2	49	500	18	metastable
	65	16 ± 3	50	400	25	metastable
	64	$16.9^{+3.9}_{-4.6}$	**140**	**140**	25	**metastable**
succinic acid	30	<0.6	44	900	–	efflorescent
	50	<0.3	51	420	–	efflorescent
	55	5.2 ± 0.3	49	530	16	metastable
	65	6 ± 1	51	470	19	metastable
	70	9 ± 3	52	450	25	metastable
	64	5.1 ± 0.8	**280**	**590**	25	**efflorescent**
glutaric acid	30	0.6 ± 0.3	51	360	4	metastable
	50	4.0 ± 0.9	56	610	8	metastable
	65	8.1 ± 0.4	53	780	14	metastable
	67	11.3 ± 2.9	**187**	**280**	**55**	**metastable**
	75	8 ± 2	46	970	16	metastable

[a] The data reported in bold type were recorded in the Large Aerosol Chamber.

TABLE 2: Uptake Coefficients for N_2O_5 Hydrolysis, γ, Obtained for Mixed Sulfate/Dicarboxylic Acid Aerosols[a]

aerosol	RH/%	$\gamma/10^{-3}$	V_a/S_a /nm	$[N_2O_5]$/ppbv	molar ratio acid:sulfate
NH_4HSO_4	60	19.6 ± 0.4	47	500	–
	60	18.7 ± 2.4	**109**	**280**	–
NH_4–oxalate	**80**	$15.5^{+4.6}_{-3.1}$	**155**	**210**	–
NH_4HSO_4/succinic acid	60	14 ± 4	58	210	1
NH_4HSO_4/glutaric acid	60	17 ± 5	59	390	1
	50	$12.0^{+0.9}_{-3.0}$	**113**	**250**	**0.9**
$(NH_4)_2SO_4$	60	16 ± 3	56	205	–
	62	$18.2^{+2.4}_{-3.0}$	**115**	**320**	–
$(NH_4)_2SO_4$/succinic acid	60	11 ± 3	60	240	1
	69	$28^{+3.6}_{-4.3}$	**141**	**125**	**0.18**
$(NH_4)_2SO_4$/glutaric acid	60	9 ± 2	57	300	1
	64	$19.8^{+2.7}_{-1.8}$	**119**	**270**	**0.38**

[a] The data reported in bold type were recorded in the Large Aerosol Chamber.

coefficient, R is the gas constant, and T is the absolute temperature. Here k_r is the first-order rate coefficient for reaction of N_2O_5 in the liquid phase and q is the reacto-diffusive parameter, defined by eq 5

$$q = r\sqrt{\frac{k^I}{D_l}} \tag{5}$$

where r is the aerosol particle radius.

At present it is not clear whether the effect of surface-active organics is to reduce the initial accommodation rate or the availability of water near the surface for the hydrolysis reaction. Diffusion of solvated molecules through the surface layer may also be slow, and the surface layer may become saturated in reactant, slowing uptake.

The current study expands this picture to include water-soluble organic acids. A detailed analysis of the uptake data presented here is made more difficult by a lack of knowledge of the physical state of the mixed organic/inorganic aerosol droplets, the rate of diffusion within the liquid medium, and the solubility of the N_2O_5. Moreover, there may be solid present, as the solubility of organic components in water varies and the organic components are more or less volatile.

4.1. The Effect of Dicarboxylic Acids on Uptake by Ammonium Sulfate and Bisulfate Aerosol. The uptake coefficients for the purely inorganic systems ammonium sulfate and ammonium bisulfate measured here are similar to those determined in earlier studies by Hallquist et al.[4] and Mentel et al.[19] As such, the data are consistent with a mass accommodation coefficient α of 0.04 and a volume-limited uptake with k_r of between 1×10^5 and 1×10^6 s^{-1}.

The effect of these organic compounds on uptake by the sulfates is much less strong than has been observed in similar studies involving surface-active organic compounds. The effect of the presence of glutaric acid on the uptake by the ammonium bisulfate aerosols is small, and the values at 50 and 60% RH agree well with measured uptake for single-component bisulfate aerosol. This is consistent with the solubility of the organic compounds in water and the formation of an internally mixed aerosol, wherein the organic and inorganic phases are well mixed.

There is a more pronounced effect of the organic acids on uptake by ammonium sulfate aerosol, although the behavior is complex. Small amounts of organic material appear to enhance, whereas larger fractions of organic matter inhibit, uptake. For instance, the reactive uptake coefficient for a 1:1 mixture of succinic acid and ammonium sulfate is smaller than that for single-component ammonium sulfate aerosol, whereas uptake by a 0.18:1 mixture is significantly larger. Similarly, reactive uptake by a 1:1 mixture of glutaric acid and ammonium sulfate is less efficient, while the 0.38:1 mixture is more efficient, in removing N_2O_5. The lower dicarboxylic acid fractions and the larger γ connected to it were measured in the static experiments in the larger chamber. As noted below, there is a possible complication due to the different mixing ratios of N_2O_5 and

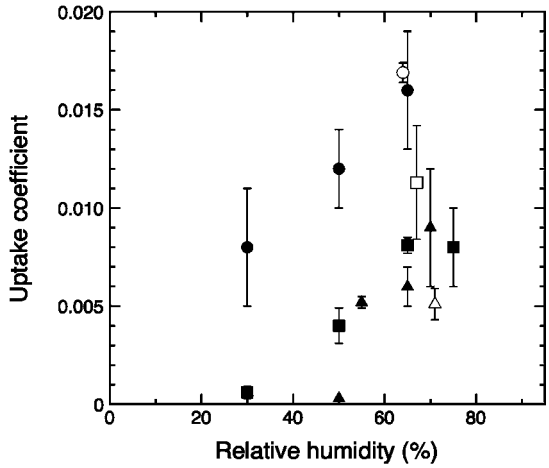

Figure 4. Uptake coefficients for loss to dicarboxylic acid aerosol as a function of relative humidty and aerosol composition. Open symbols: chamber measurements. Filled symbols: aerosol flow tube measurements. ○, malonic acid; Δ, succinic acid; □, glutaric acid.

different contact times used in the experiments. On the other hand, the largest uptake coefficient 0.028 is indeed observed for the substrate with the lowest dicarboxylic acid to sulfate ratio of 0.38. From the data set, it is clear that the opposing trends indicate a complex behavior in the uptake processes.

4.2. Effect of Particle Phase on Uptake of N_2O_5 by Dicarboxylic Acid Aerosol. Loss of N_2O_5 onto solid aerosol has been shown to proceed more slowly than loss to liquids droplets.[12,19] In the case of succinic acid, no uptake was measurable using the aerosol flow tube reactor below 55% RH. Above this point, uptake proceeds with moderate efficiency, comparable to that of glutaric acid. The efflorescence point of succinic acid is 53% RH,[20] and below this point the liquid aerosols prepared by the atomizer probably exist as solid particles and reactive uptake is much less efficient than onto liquid particles.[4,19]

The very small uptake coefficients shown by solid particles explain also the lower uptake onto succinic acid and oxalic acid aerosol observed in the large aerosol chamber experiments compared to the flow tube measurements. For oxalic acid the drying process was manifest not only in γ but also by the shift and sharpening of the IR band in the range of 1180−1280 cm^{-1} (Figure 5). Within the chamber there is a slight negative vertical temperature gradient, which promotes circulation, but which produces lower RH near the floor of the chamber compared to near the ceiling. As the aerosol circulates, it may effloresce on reaching the lower RH portion of the aerosol chamber. Oxalic and succinic aerosols have efflorescence points close to the RH in the chamber, and this may well result in their eflorescene on passing over the warmer floor of the aerosol chamber. This would lead to a time-varying external mixture of solid and liquid aerosol particles. As a result the average measured uptake coefficient, being an average of uptake onto the two types of particles, is lower than that onto entirely liquid particles determined in the flow tube studies.

4.3. Effect of Particle Size and Water Content on Uptake of N_2O_5 by Dicarboxylic Acid Aerosol. In the case of slow rate of reaction relative to the rate of diffusion in solution, and fast mass accommodation, the uptake is limited by the aerosol volume and eq 4 reduces to eq 6

$$\frac{1}{\gamma} = \frac{1}{\alpha} + \frac{\nu}{4K_H RTk_r}\frac{S_a}{V_a} \tag{6}$$

where S_a is the aerosol surface area and V_a is the aerosol volume.

For a fast reaction in the condensed phase relative to diffusion, the uptake coefficient is given by the size-independent expression, eq 7:

$$\frac{1}{\gamma} = \frac{1}{\alpha} + \frac{\nu}{4HRT\sqrt{k_r D_l}} \tag{7}$$

Thus, as particle size increases, a transition from the size-dependent to the size-independent regime is expected. The point at which this transition occurs is dependent on the physicochemical parameters governing uptake.

If the concentration of nitrate within the aerosol is zero, k_r is the first-order rate coefficient for reaction between N_2O_5 and water in the condensed phase, i.e. $k_r = k^{II}[H_2O]$, where k^{II} is a bimolecular reaction rate coefficient. Thus, for volume-limited uptake

$$\gamma = \frac{4K_H RTk^{II}[H_2O]}{c}\frac{S_a}{V_a} \tag{8}$$

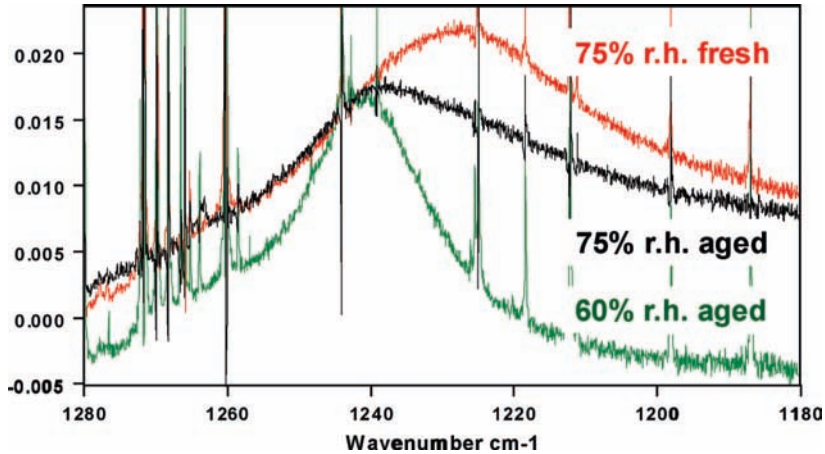

Figure 5. IR spectra of oxalic acid aerosol (C═O stretch range) in fresh and aged state at 75% RH and aged state at 60% RH as observed in the Aerosol Chamber in Juelich. Aging narrows and blue shifts the absorption band, indicating drying of the particles. Uptake coefficients of N_2O_5 for both aged aerosols are given in Table 1.

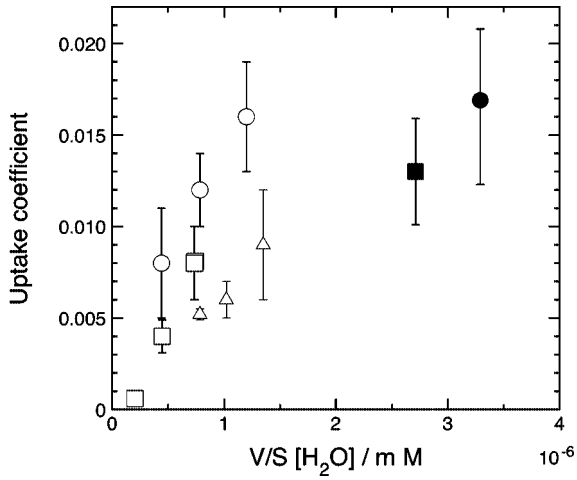

Figure 6. Dependence on uptake coefficient on particle size and water content, using eq 8. Filled symbols: chamber measurements. Open symbols: aerosol flow tube measurements. ○, malonic acid; Δ, succinic acid; □, glutaric acid.

Figure 6 shows a plot of the uptake coefficient against $[H_2O]V_a/S_a$. $[H_2O]$ was calculated using the data of Peng et al. and the known densities of malonic, succinic, and glutaric acids,[21] assuming linear dependence of aerosol density on aerosol mass fraction solute. The chamber data for succinic acid and oxalic acid are omitted from the plot for reasons discussed above.

As can be seen, while an approximately linear behavior is observed at low $[H_2O]V_a/S_a$, indicating volume-limited uptake, the rate of increase decreases significantly above approximately 1 M μm, consistent with a reacto-diffusive length at 50% RH of less than 50 nm given an average particle diameter of the surface size distribution in the chamber measurements of about 600 nm. It is apparent from the figure that the reactivity of the aerosol is not controlled solely by aerosol water content and particle size. From a fit of the low V_a/S_a data of Figure 6 to eq 8, values of k^{II} of 1.8×10^4, 7.9×10^3, and 1.2×10^4 M^{-1} s^{-1} are found for malonic, succinic, and glutaric acids, respectively, indicating that additional factors control the reactivity.

4.4. Effect of N_2O_5 Mixing Ratio on Retrieved Uptake Coefficients. Wahner et al. demonstrated that the uptake coefficient decreases with increasing nitrate activity in the aerosol droplet and proposed a mechanism involving a reversible reaction of dissolved N_2O_5 with water to make nitrate and hydrated nitronium ions.[18]

Although nitrate effect was initially identified from the study of the RH dependence of uptake onto sodium nitrate aerosol, as Thornton et al. noted, this nitrate effect can also be manifest as a decreasing uptake coefficient with increasing partial pressure of N_2O_5.[12] This is because as N_2O_5 is hydrolyzed, the concentration of nitric acid and the nitrate ion in the aerosol increases, and further uptake is inhibited. Indeed, Thornton et al. observed a small negative dependence of uptake coefficient on partial pressure of N_2O_5 over the range 6−28 ppbv mixing ratio which they attributed to this nitrate effect.[12] In the measurements reported here, significantly higher mixing ratios of $N_2O_5 > 100$ ppbv were employed compared to the 6−30 ppbv employed in the work of Thornton et al. The use of higher mixing ratios could mean that the reaction product, the nitrate ion, may build up to levels sufficient to significantly inhibit uptake. In order to examine whether this was the cause of the discrepancy between the two studies, we developed a numerical model of uptake to investigate the effect of N_2O_5 mixing ratio and nitrate concentration on uptake.

4.5. Reacto-Diffusive Model of Uptake. The model employs a coupled treatment of reaction and diffusion in the aerosol droplet, taking as a mechanism reactions 3−9 thereby including reaction of N_2O_5, HNO_3 in gas and condensed phases, and ionic species NO_2^+ and NO_3^-. It simulates concentration of both gas-phase and liquid-phase species. The model is written using Mathematica and solved via NDSolve routines.

In the model, the aerosol particles are treated as a series of concentric equal-volume aqueous shells, and diffusion between them is parametrized using transfer coefficients derived from the diffusion coefficients of individual species. Calculations of reaction rates within the aerosol volume are performed on a concentration, rather than activity, basis, and for a single-particle radius, chosen to be the effective aerosol radius, $3V_a/S_a$.

Transfer between the gas and liquid phases proceeds at a rate determined by the mass accommodation coefficient, α, and the Henry's Law coefficient, K_H. The reaction equation describing the outer shell is therefore

$$\frac{d[N_2O_5]_{(0)}}{dt} = T_1([N_2O_5]_{(1)} - [N_2O_5]_{(0)}) + k_3[N_2O_5]_{(g)} - k_4[N_2O_5]_{(0)} - k_5[N_2O_5]_{(0)} + k_6[NO_2^+]_{(0)}[NO_3^-]_{(0)} \quad (9)$$

where

$$k_3 = \alpha\frac{c}{4}S_a \quad (10)$$

and

$$k_4 = \frac{k_3}{K_{H,N_2O_5}} \quad (11)$$

and where the subscripts in the concentration terms refer to an individual shell—0 being the outermost shell. The concentration of N_2O_5 is calculated in units of mol dm^{-3} (M). K_{H,N_2O_5} is chosen to be 5.0 M atm^{-1}, equivalent to 2.0×10^{-19} M cm^{-3}. The transfer coefficients, T, describe diffusion between the different shells of the spherically symmetrical droplet.

Within the aerosol droplet, the equations are

$$\frac{d[N_2O_5]_{(i)}}{dt} = T_i([N_2O_5]_{(i)} - [N_2O_5]_{(i+1)}) - T_{i-1}([N_2O_5]_{(i-1)} - [N_2O_5]_{(i)}) + k_5[N_2O_5]_{(i)} + k_6[NO_2^+]_{(i)}[NO_3^-]_{(i)} \quad (12)$$

Similar expressions apply to the concentration of HNO_3, while only reaction and diffusion are used to describe NO_2^+ and NO_3^-. Figure 7 shows a simulation of uptake by malonic acid aerosol, for conditions of aerosol volume and N_2O_5 mixing ratio representative of an uptake experiment at 70% RH: the removal of N_2O_5 and simultaneous appearance of HNO_3 in the gas phase and nitrate in the condensed phase agree well with the qualitative features of our experiments. Uptake coefficients were derived from the calculated rate of disappearance of N_2O_5 from the gas phase. To do this, the model was run for 15 s experimental (model) time and the calculated N_2O_5 concentrations were fit to a single-exponential, i.e., first-order, decay. The derived rate coefficient was then used to obtain an uptake coefficient using eq 1.

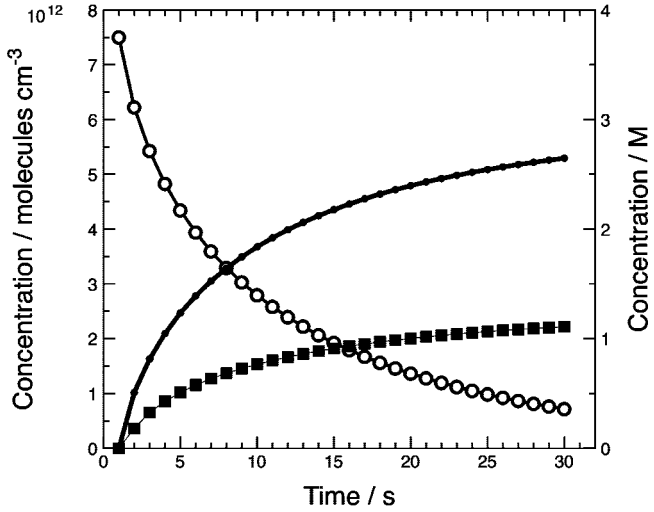

Figure 7. Simulated time dependence of N_2O_5, HNO_3, and particle-phase nitrate concentrations in an AFT experiment. Particle size (V/S) = 300 nm, N_2O_5 mixing ratio of 300 ppbv, and physicochemical parameters such as $[H_2O]$ and diffusion coefficient appropriate to malonic acid at 70% RH. ○, gas-phase N_2O_5 concentration; ■, HNO_3 concentration; ●, NO_3^- concentration in aerosol volume.

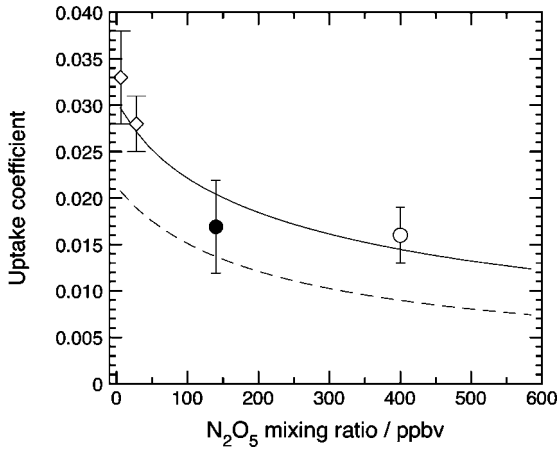

Figure 8. Comparison between experimentally measured and calculated uptake coefficient for malonic acid at 70% RH. The lines show the dependence of uptake coefficient on mixing ratio of N_2O_5; the points are experimental data.

Figure 8 shows a plot of these simulated uptake coefficients as a function of N_2O_5 mixing ratio together with experimentally determined uptake coefficients. The data of Thornton et al. is also plotted. All experimental data are uptake coefficients measured between 65 and 70% RH, where there is good overlap between the two aerosol flow tube studies and the aerosol chamber measurements. Calculations were performed for a relative humdity of 70%, using water concentrations estimated from the data of Peng et al.[21]

The figure shows that the simulated uptake coefficients are sensitive to the concentration employed in the gas phase. This is ascribed to the gradual buildup of nitrate within the aerosol volume as uptake proceeds and increasing rate of reaction R6. This has the effect of reducing the simulated rate of uptake and the derived uptake coefficient. Figure 8 shows simulations using two sets of kinetic parameters. The broken line shows a simulation using a value for k_6 of 8×10^5 s^{-1}, derived using eq 6, and a ratio $k_6/k_7[H_2O]$ of 10, derived by Wahner et al. from their study of the uptake of N_2O_5 by sodium nitrate aerosol.[18]

The model does a satisfactory job of reproducing the observed uptake coefficients using these parameters, as indicated by the broken line in Figure 8. The solid line shows a simulation using the same parameters, except that k_5 was increased to 5×10^6 s^{-1}, in line with Wahner et al. and Mentel et al.[4,22] While the agreement with the data of Thornton et al. is improved, a somewhat higher sensitivity to the nitrate concentration is required to reproduce the experimental data than that inferred by Wahner et al. In the simulation shown, a value of 30 was chosen for the ratio $k_6/k_7[H_2O]$.

The best value of k_5 is somewhat higher than that derived from application of eq 6 for volume-limited uptake of 8×10^5 s^{-1}. This is probably due to the inclusion of the effects of solubility and diffusion in this numerical treatment of the uptake process. The solubility of N_2O_5 in aqueous media is rather low, estimated at around 5 M atm^{-1}, and it is to be expected that, unless the transport within the droplet is rapid, the outermost layer will quickly saturate with N_2O_5 and the observed rate of uptake will decrease. In fact, we did observe that as the diffusion coefficient is increased in the simulations, the limiting value of the reactive uptake coefficient at low mixing ratio increased. This supports the idea that there is fast saturation of the outermost layer of the aerosol particle with N_2O_5 compared to the time scale of diffusive transport within the droplet.

For these physicochemical parameters, the uptake process is not entirely volume-limited and any value of k_5 derived from an analysis based on volume-limited uptake will be too low. On the other hand, as the diffusion coefficient increases over the range $1 \times 10^{-6} - 1 \times 10^{-4}$ cm^2 s^{-1}, the calculated reactive uptake coefficient increased by approximately a factor of 2. Therefore the uptake process conforms partially to surface-limited kinetics, and the choice of diffusion coefficient is a significant source of uncertainty in these simulations. Given the good agreement observed here between model and observations, and until such times as accurate values of D_l are available, we proceeded on the basis of a liquid-phase diffusion coefficient of 1×10^{-5} cm^2 s^{-1}. This reproduced the measured uptake coefficients well using the parameters above.

There is a close similarity similarity between the parameters derived from a study of uptake to sodium nitrate aerosol[22,4] and those inferred here. We conclude that that the water-soluble acids have little effect on uptake. At low N_2O_5 mixing ratio or low nitrate concentrations, the uptake process is accommodation-limited. However, on the basis of the mechanism presented here, the rate of reactive uptake is quite sensitive to the nitrate concentration within the aerosol, and at around 1 M, the uptake coefficient is reduced by 50%.

4.6. Analysis of Kinetics of Uptake to Other Dicarboxylic Acid Aerosol. A similar analysis of the data describing uptake by the succinic and glutaric acid aerosol is made more difficult due to the lack of measurements at low N_2O_5 mixing ratio to constrain k_5. However, these data may be shown to form a consistent set with the malonic acid data set.

To do this, we employed a second method of analysis in which we again assumed that the nitrate concentration increases within the aerosol following uptake and hydrolysis of N_2O_5. This occurs during the time taken for gas and aerosol to become completely mixed. Using reactions 5−7 given above, putting the concentration of NO_2^+ into steady state results in an expression for the first-order rate coefficient of hydrolysis within the aerosol volume, k_r, of the form

$$k_r = k_5\left(1 - \frac{k_6[NO_3^-]}{k_6[NO_3^-] + k_7[H_2O]}\right) \qquad (13)$$

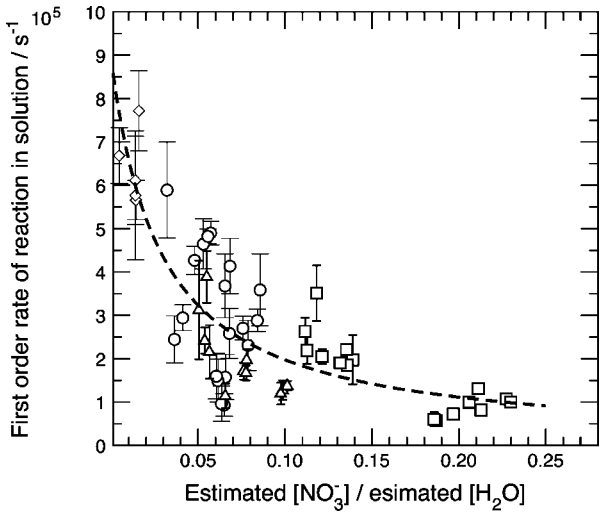

Figure 9. Dependence of liquid phase reaction rate coefficient on $[NO_3^-]$ and $[H_2O]$. Data are from aerosol flow tube measurements: ◇, Thornton et al.;[12] ○, malonic acid; Δ, succinic acid; □, glutaric acid.

in which the rate coefficient decreases with increasing nitrate concentration. As mentioned in the experimental section, the gas and aerosol require around 5 s to mix completely. The nitrate concentration in the aerosol was therefore estimated by assuming that uptake at first proceeds at an accommodation-limited rate (i.e., $\gamma = 0.04$ and using the experimentally determined surface area) during 5 s of contact between aerosol and gas. As a result, this calculation reflects an upper limit of $[NO_3^-]$ in the aerosol at the point at which measurement commences.

The HNO_3 produced is then partitioned between gas and condensed phases according to the pH-dependent solubility of the HNO_3.[23] Our estimate of pH uses the calculated aerosol liquid water content and volume and acid pK_a, and the calculation of $[NO_3^-]$ employs an iterative method similar to that described in Thornton et al.[12] The calculated nitrate concentrations were in the range 0.5−2 M. This range is consistent with observations made in the chamber measurements, in which the concentration of particulate nitrate was found to be 0.1 (malonic) to 2.7 (glutaric) mol kg^{-1}.

Using eq 6, and the known aerosol water content, the first-order rate coefficient for reaction in solution may be obtained from the measured uptake coefficient and eq 6. For this analysis, in keeping with the analysis of Thornton et al., we have assumed that the mass accommodation step does not affect the kinetics of uptake.

Figure 9 shows a plot of these data against the ratio of nitrate ion to water concentration in the aerosol volume. From a fit of the rate law given in eq 13, the rate coefficients k_5 and the ratio k_6/k_7 may be obtained. Figure 9 shows a plot of the data, including that obtained by Thornton et al., and a fit to the expression for volume-limited uptake employed in that work. From the fit, we obtain values of k_5 of 8×10^5 s^{-1} and a ratio of rate coefficients k_6 to k_7 of approximately 30 in agreement with our analysis using a more explicit treatment of aerosol processes. A similar analysis including the effect of mass accommodation rate yields a value of k_5 of 5×10^6 s^{-1}, consistent with our more detailed analysis.

5. Conclusions and Summary

We have made the first study of the effect of dicarboxylic acids on uptake by sulfate aerosols. In contrast to surface-active organics, only a small effect is observed of these acids on uptake by sulfate aerosol. This is the first study of uptake onto oxalic succinic and glutaric, and similar uptake coefficients onto liquid aerosol are observed. Below the crystallization point of the aerosol, we observed reduced uptake.

We have observed the effect of increased levels of N_2O_5 on uptake which has been rationalized on the basis of the nitrate effect, and the combined effects of particle size, water content, and pH-dependent partitioning of HNO_3 hydrolysis product.

On the basis of our results we recommend a parametrized form for uptake coefficient to include the effect of nitrate concentration on uptake. Using the data given

$$k_r = k_5\left(\frac{k_6[NO_3^-]}{k_6[NO_3^-] + k_7[H_2O]}\right) \qquad (14)$$

with $k_5 = 5 \times 10^6$ s^{-1} and the ratio k_6 to $k_7 = 30$.

Acknowledgment. This work is part of the CASOMIO project and is supported by the EC (Contract No. EVK2-CT-2001-00124). The support of the UK National Centre for Atmospheric Science is acknowledged for P.T.G., as well as the ESF INTROP scheme for support for travel.

References and Notes

(1) Hu, J. H.; Abbatt, J. P. D. *J. Phys. Chem. A* **1997**, *101* (5), 871–878.
(2) Mozurkevich, M.; Calvert, J. G. *J. Geophys. Res.—Atmospheres* **1988**, *93*, 15889–15896.
(3) Hallquist, M.; Stewart, D.; Baker, J.; Cox, R. *J. Phys. Chem. A.* **2000**, *104*, 3984–3990.
(4) Hallquist, M.; Stewart, D.; Stephenson, S.; Cox, R. *Phys. Chem. Chem. Phys.* **2003**, *5*, 3453–3463.
(5) George, C.; Ponche, J. L.; Mirabel, P.; Behnke, W.; Scheer, V.; Zetzsch, C. *J. Phys. Chem.* **1994**, *98*, 8780–8784.
(6) Wahner, A.; Mentel, T. F.; Sohn, M.; Stier, J. *J. Geophys. Res.* **1998**, *193* (D23), 31103–31112.
(7) Folkers, M.; Mentel, T.; Wahner, A. *Geophys. Res. Lett.* **2003**, *30* (12).
(8) McNeill, V. F.; Wolfe, G. M.; Thornton, J. A. *J.Phys. Chem. A* **2007**, *111* (6), 1073–1083.
(9) Badger, C.; George, I.; Griffiths, P.; Abbatt, J.; Cox, R. *J. Phys. Chem. A.* **2006**, *110*, 6986.
(10) Park, S.-C.; Burden, D. K.; Nathanson, G. M. *J. Phys. Chem. A.* **2007**, *111* (15), 2921–2929.
(11) Anttila, T.; Kiendler-Scharr, A.; Tillmann, R.; Mentel, T. F. *J. Phys. Chem. A.* **2006**, *110* (35), 10435–10443.
(12) Thornton, J. A.; Braban, C. F.; Abbatt, J. P. D. *Phys. Chem. Chem. Phys.* **2003**, *5* (20), 4593–4603.
(13) Kawamura, K.; Narukawa, M.; Li, S. M.; Barrie, L. A. *J. Geophys. Res.—Atmospheres* **2007**, *112* (D10).
(14) Mentel, T. F.; Bleilebens, D.; Wahner, A. *Atmos. Environ.* **1996**, *30* (23), 4007–4020.
(15) Grimalt, J. O.; Olive, J. *Anal. Chim. Acta* **1991**, *248* (1), 59–70.
(16) Tang, I. N. *J. Geophys. Res.—Atmospheres* **1996**, *101* (D14), 19245–19250.
(17) Brown, R. *J. Bur. Natl. Standards* **1978**, *83*, 1–8.
(18) Robinson, G. N.; Worsnop, D. R.; Jayne, J. T.; Kolb, C. E.; Davidovits, P. *J. Geophys. Res.* **1997**, *102* (D3), 3583–3602.
(19) Folkers, M.; ten Brink, H.; Mentel, T.; Cox, R. Heconos final report, ec contrac env4-ct97-0407, Technical report, 2001.
(20) Braban, C. F.; Carroll, M. F.; Styler, S. A.; Abbatt, J. P. D. *J.Phys. Chem. A* **2003**, *107* (34), 6594–6602.
(21) Peng, C.; Chan, M. N.; Chan, C. K. *Environmental Sci. Technol.* **2001**, *35* (22), 4495–4501.
(22) Mentel, T.; Sohn, M.; Wahner, A. *Phys. Chem. Chem. Phys.* **1999**, *1*, 5451–5457.
(23) Seinfeld, J. H.; Pandis, S. N. *Atmospheric Chemistry and Physics: from Air Pollution to Climate Change*; Wiley: New York, 1998.

JP8096814